Available online at www.sciencedirect.com
ScienceDirect
Russian Geology and Geophysics 48 (2007) 523–531
RUSSIAN GEOLOGY AND GEOPHYSICS
www.elsevier.com/locate/rgg

Electromagnetic processes in a conducting magnetic casing string

M.I. Epov *, G.M. Morozova, E.Yu. Antonov

Institute of Petroleum Geology and Geophysics, Siberian Branch of the RAS, 3 prosp. Akad. Koptyuga, Novosibirsk, 630090, Russia

Received 17 October 2005

Abstract

We investigated the electromagnetic filed of a current loop in a conducting ferromagnetic cylinder for applications of casing monitoring in petroleum wells. We tested different transmitter-receiver configurations for excitation and recording of TEM and stationary magnetic fields, studied the responses to changes in electromagnetic and geometrical parameters of casing strings, and determined the intervals of highest sensitivity.

Keywords: Transient electromagnetic field; resistivity; ferromagnet; magnetic permeability

Introduction

Earlier we (Epov et al., 2002; Morozova et al., 2000) reported a solution for the TEM response of a current loop in a conducting cylindrical layered ferromagnet and the final equation for emf excited in a receiver loop placed on the cylinder axis. The solution was used to design a downhole flaw detector for condition monitoring of petroleum well casing.

In the cited works we investigated the behavior of emf in response to changing electromagnetic parameters and geometry of casing, but some essential features of the transient process and related instrumental and methodological solutions remained unexplored. Namely, the distribution of eddy current over the string, required to constrain the depth interval in real configurations, the screening capacity of the highly conducting magnetic inner string in multistring casing, etc. In this study we derive equations for magnetic induction components to estimate the intensity of magnetizing field, its pattern and direction within the peak interval. The available algorithms allowed us to investigate the harmonic TEM and stationary magnetic field and their responses to changes in model electromagnetic (magnetic permeability and resistivity) and geometrical (inner and outer radii) parameters, and to assess the applicability of the method.

Following the problem formulation and solutions from (Morozova et al., 2000), we cite equations for the TEM field components for the three domains of the model (Fig. 1): nonconducting nonmagnetic inner cylinder ($r < r_1$, domain 0), cylindrical conducting ferromagnetic casing ($r_1 \le r \le r_2$, domain 1), and the nonconducting nonmagnetic formation outside the cylinder ($r > r_2$, domain 2). The simulated configuration includes two transmitter loops with their centers T_1 and

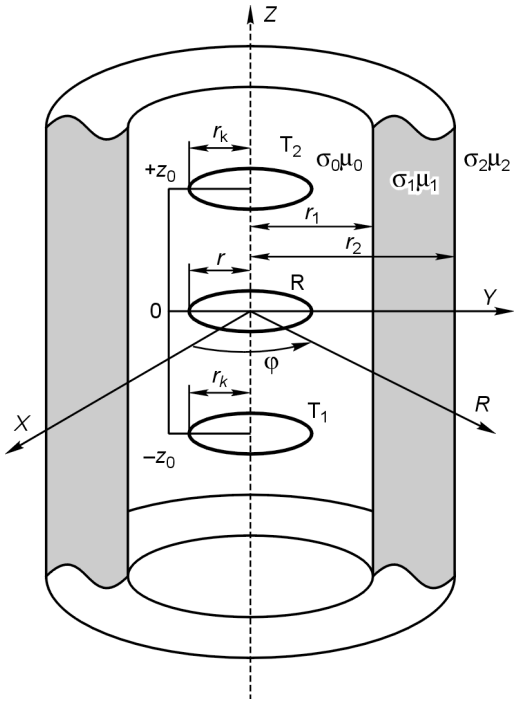

Fig. 1. Model of medium and experimental layout. See text for explanation.

* Corresponding author.
E-mail address: epov@emf.ru (M.I. Epov)

1068-7971/$ - see front matter © 2007, IGM, Siberian Branch of the RAS. Published by Elsevier B.V. All rights reserved.
doi:10.1016/j.rgg.2007.06.011

T_2 on the symmetry axis of a cylindrical casing string, and a receiver loop R, likewise in a horizontal plane. Series or counter direct current I in the transmitter loops is turned off at $t = 0$. The origin of the cylindrical coordinates coincides with the center of the receiver loop (Fig. 1).

To obtain realistic estimates, we used resistivity and magnetic permeability of real casing strings measured in laboratory.

The metal casing string is assumed to be ferromagnetic (Vonsovsky and Shur, 1948). Ferromagnetic materials have an extremely high field-dependent magnetic susceptibility. Their magnetic permeability is nonlinearly related to the external magnetic field and is a multi-valued function controlled by the prehistory of the sample which can have remanent magnetization.

In our case remanent magnetization can be produced by the temperature conditions of string rolling. The problem is solved under the assumption that the string is uniformly magnetized while the magnetic induction and the magnetic field are linearly related as $\mathbf{B} = \mu\mathbf{H}$, which works for low magnetic fields.

Structure of the EM field

The electromagnetic field components in the three domains are (Morozova et al., 2000):

$$E_\varphi = \frac{M}{2\pi^2}\int_0^\infty F(r, t, \lambda)\cos(\lambda z)d\lambda,$$

$$H_r = \frac{M}{2\pi^2}\int_0^\infty R(r, t, \lambda)\sin(\lambda z)d\lambda, \quad (1)$$

$$H_z = \frac{M}{2\pi^2}\int_0^\infty Z(r, t, \lambda)\cos(\lambda z)d\lambda.$$

The Fourier images F, R, and Z are related as

$$\lambda R - \frac{\partial Z}{\partial r} = \sigma F,$$

$$-\lambda F = \mu\frac{\partial R}{\partial t},$$

$$\frac{1}{r}\frac{\partial(rF)}{\partial r} = -\mu\frac{\partial Z}{\partial t}, \quad (2)$$

$$\frac{1}{r}\frac{\partial(rR)}{\partial r} = \lambda Z.$$

The problem is formulated for the R Fourier image, the component of the magnetic field H_r normal to the interfaces μ and σ. The function R is sought as superposed solutions of the form $R = X(r)e^{-\alpha t}$.

Let the problem be confined to the domain of the cylinder itself $r_1 \le r \le r_2$. Using the boundary conditions and the solution dependence on the space coordinate outside the cylinder walls, we obtain the Sturm-Liouville problem for $X(r)$.

$$r^2X_{rr}'' + \frac{X_r'}{r} + (m^2x^2 - 1)X = 0;$$

$$X + r_1X_r' = a_1X, \quad r = r_1;$$

$$X + r_2X_r' = -a_2X, \quad r = r_2.$$

According to the superposition principle, the general solution for R is

$$R(r, t) = \sum_{j=0}^{\infty} C_j X_j(r)\cdot e^{-\alpha_j t},$$

where X_j are the eigenfunctions of the Sturm-Liouville problem and $X_j = A\cdot J_1(m_j\bar{r}) + BN_1(m_j\bar{r})$ and m_j are the eigenvalues, $\bar{r} = r/r_1$, $\alpha_j = \dfrac{m_j^2 + q^2}{\mu_1\sigma_1 r_1^2}$.

The coefficients A and B are

$$A = N_0(m_j) - \bar{a}_1N_1(m_j),\ B = -J_0(m_j) + \bar{a}_1J_1(m_j),$$

where $J_1(x)$ and $N_1(x)$ are the first-order Bessel and Neumann functions, respectively,

$$\bar{a}_1 = \bar{\mu}\frac{q_1}{m_j}\frac{I_0(q_1)}{I_1(q_1)},\ \bar{a}_2 = \bar{\mu}\frac{q_1}{m_j}\bar{r}_2\frac{K_0(q_1\bar{r}_2)}{K_1(q_1\bar{r}_2)},$$

$$\bar{\mu} = \mu_1/\mu_0,\ q_1 = \lambda r_1,\ \bar{r}_2 = r_2/r_1,$$

and $I_n(x)$ and $K_n(x)$ are the modified Bessel functions. The coefficients C_j were determined using the initial conditions and the orthogonality of the eigenfunctions X_j with the weight r.

$$C_j = \frac{q_1^2}{r_1^2m_j^2 + q_1^2}\cdot\frac{P_j}{Q_j},$$

where

$$Q_j = \frac{1}{2}X_j^2(m_j\bar{r}_2)(\bar{r}_2^2 + \bar{a}_2^2 + 2\bar{a}_2/m_j) -$$

$$\frac{1}{2}X_j^2(m_j)(1 + \bar{a}_1^2 - 2\bar{a}_1/m_j).$$

P_j is given by

$$P_j = \{A\bar{A}^*f_3 + B\bar{A}^*f_4 - A\bar{B}^*f_5 - B\bar{B}^*f_6\}|_{r_1}^{r_2},$$

where

$$f_3 = qJ_1(m_j\bar{r})I_0(q) - m_j\bar{r}J_0(m_j\bar{r})I_1(q),$$

$$f_4 = qN_1(m_j\bar{r})I_0(q) - m_j\bar{r}N_0(m_j\bar{r})I_1(q),$$

$$f_5 = qJ_1(m_j\bar{r})K_0(q) - m_j\bar{r}J_0(m_j\bar{r})K_1(q),$$

$$f_6 = qN_1(m_j\bar{r})K_0(q) - m_j\bar{r}N_0(m_j\bar{r})K_1(q),$$

$$\bar{r} = r/r_1,\ q = \lambda r,\ \bar{A}^* = -\bar{B}^*f_1 - f_2,$$

$$f_1 = \frac{\mu \cdot I_0(q_1)\, K_1(q_1) + I_1(q_1)\, K_0(q_1)}{I_1(q_1)\, I_0(q_1)\, (\bar{\mu} - 1)}, \quad f_2 = \frac{1}{q_1 I_1(q_1)\, I_0(q_1)\, (\bar{\mu} - 1)},$$

$$\bar{B}^* = \frac{f_2 [I_0(q_2)\, K_1(q_2) + \bar{\mu} K_0(q_2)\, I_1(q_2)]}{K_0(q_2)\, K_1(q_2)\, (\bar{\mu} - 1) - f_1 [I_0(q_2)\, K_1(q_2) + \bar{\mu} K_0(q_2)\, I_1(q_2)]}.$$

The solution for the radial magnetic field component, according to (1), is

$$H_r = \frac{M}{2\pi^2 \cdot r_1^3} \int_0^\infty \sin(m_j \bar{z}) \sum_{j=0}^\infty X_j(m_j \bar{r}) \frac{q_1^2}{m_j^2 + q_1^2} \frac{P_j}{Q_j} e^{\frac{-(m_j^2 + q_1^2)t}{r_1^2 \mu_1 \sigma_1}} dq_1. \quad (3)$$

All other components and their time derivatives inside the cylinder ($r_1 \le r \le r_2$) can be easily obtained from (1) and (2).

Field inside the cylinder ($r < r_1$). According to the conditions at the interfaces and the derivation in (Epov et al., 2002), the radial magnetic field component inside the cylinder is

$$H_r = \frac{M}{2\pi^2 \cdot r_1^3} \bar{\mu} \int_0^\infty \frac{I_1(q_1 \bar{r})}{I_1(q_1)} \sin(q_1 \bar{z}) \times$$

$$\sum_{j=0}^\infty X_j(m_j) \frac{q_1^2}{m_j^2 + q_1^2} \frac{P_j}{Q_j} e^{\frac{-(m_j^2 + q_1^2)t}{r_1^2 \mu_1 \sigma_1}} dq_1. \quad (4)$$

All notations in (4) were explained above. As in the previous case, the other components of the EM field are found from (1) and (2).

Field outside the cylinder ($r > r_2$). The magnetic field radial component outside the cylinder is

$$H_r = \frac{M}{2\pi^2 \cdot r_1^3} \int_0^\infty \sin(q \bar{z}) \frac{K_1(q_1 \bar{r})}{K_1(q_2)} \times$$

$$\sum_{j=0}^\infty X_j(m_j \bar{r}) \frac{q_1^2}{m_j^2 + q_1^2} \frac{P_j}{Q_j} e^{\frac{-(m_j^2 + q_1^2)t}{r_1^2 \mu_1 \sigma_1}} dq_1. \quad (5)$$

The other components of the EM field are found therefrom in the same way as above.

emf behavior at different parameters of real string samples

The model of a uniform string has two electromagnetic parameters μ and ρ and two geometrical parameters r_1 and r_2, the inner and outer radii, respectively. The magnetic permeability μ and resistivity ρ are not the sought parameters in the inversion but they should be known as they control the electrodynamic process, especially diffusion and decay of the induction current in the cylinder wall which, in turn, is essential for estimating wall thickness and for discriminating the elements of multistring casing.

The resistivity of string samples measured in laboratory (Epov et al., 2003a) varied within 1–2% in different samples and was $2.2 \cdot 10^{-7}$ Ohm·m on average at 20 °C. Therefore, the string resistivity can be assumed invariable in calculations and log data interpretation. Magnetic permeability measurements showed different remanent magnetizations in different string segments, but the scatter reduced considerably if the samples were demagnetized prior to the measurements. The average magnetic permeability over all samples was $100.5\mu_0$, with a rms error of $\pm 7.96\mu_0$. The large μ variance influences greatly the measured emf. Therefore, magnetic permeability, as well as the radii, is to be estimated from measurements rather than being specified in advance. However, we assume hereafter that magnetic permeability is rather uniform within a string segment.

Diffusion of induction current

The response of the recorded field to changes in string magnetic permeability and wall thickness largely depends on distribution of induction current in the walls. For instance, the depth z is controlled by the rate of current diffusion along the string height and radius.

Hereafter we use the absolute time because the time interval is actually independent of small size and resistivity variations. It is convenient to describe the diffusion of induction current using its density contour lines. In Fig. 2 diffusion is shown inside a 10 mm thick string at 0.3, 5, and 80 ms, the periods commonly used in downhole flaw detectors (Martynov et al., 1999).

Note first of all that at early times current spreads over the conductor surface as $z \approx \pm 0.1$ m and penetrates to about 1 mm (t = 0.3 ms). Therefore, the signals at times less than 1 ms can be used for flaw detection in the inner string wall and for estimating the inner radius, i.e., the times before 1 ms are good for monitoring the inner wall and its thickness. In practice, the possibility to detect flaws smaller than the diffusion area depends on the current contribution into the measured signal.

Current penetrates the wall through at times greater than 5 ms. Then the current density maximum moves to the outer wall and current becomes more uniformly distributed. After 10 ms the greatest portion of current is symmetrical over the wall thickness (h) and the recorded emf depends uniquely on h (Fig. 2, *b–d*). The depth of current diffusion is smaller at greater μ. The thickness of the string wall is averaged over an interval of $z \approx 0.05$ m at a cable length of $2z_0 = 0.029$ m (Fig. 1).

Magnetic field in string walls and behavior of its radial component at different string parameters

The behavior and structure of the magnetizing field show up in the distribution of its components in the string walls.

The contour line pattern of H_z is the same as in j_φ (Fig. 2). The contour lines of H_r are distributed more uniformly over

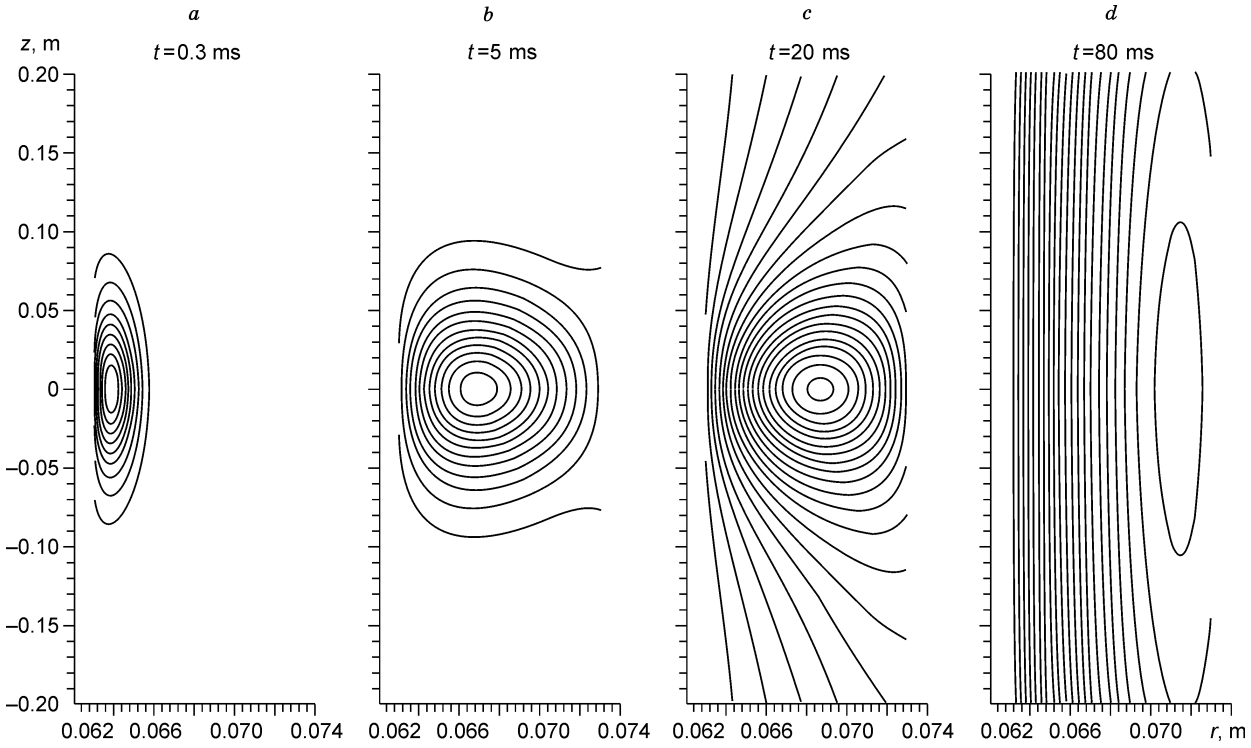

Fig. 2. Current density contour lines j_φ (A/m^2) in a ferromagnetic conductor at $\mu = 100$.

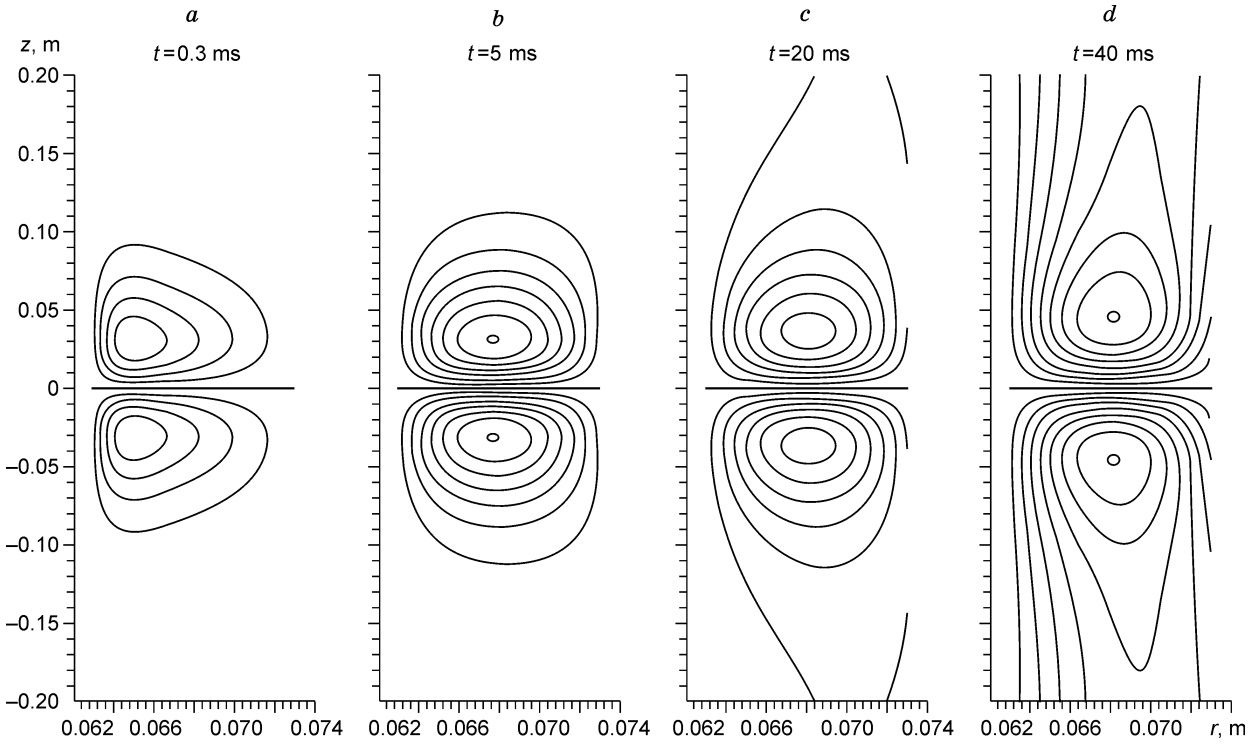

Fig. 3. H_r contour lines (A/m) in a ferromagnetic conductor at $\mu = 100$.

the wall thickness (Fig. 3). Already at 5 ms, the pattern is almost symmetrical about the center, and the symmetry holds as far as the latest times (40 ms). If the maximum H_z is at the transmitter depth, the coordinates of H_r extremes move along z from $z = \pm 0.3r_1$ at $t = 0.3$ ms to $z = \pm 0.5r_1$ at $t = 40$ ms. Inasmuch as the vertical component approaches zero and the radial component is the greatest at $z \cong \pm 0.5r_1$, the direction of the magnetic field changes from the vertical at the source depth to almost radial at $z \cong \pm 0.5r_1$.

Note that the TEM field causes no measurable magnetiza-

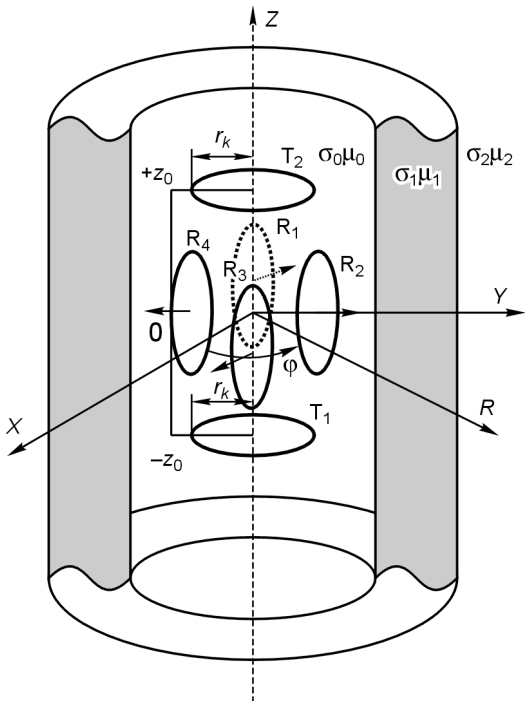

Fig. 4. Transmitter-receiver configuration with horizontal loops. See text for explanation.

tion of strings. Indeed, the greatest emf at early times for the instrument we discuss is about 1 mV (Epov et al., 2002), which corresponds to the magnetic field $H_z \sim 5$ A/m. This field is typical of the initial segment of the hysteresis loop where the processes are reversible (Vonsovsky and Shur, 1948). We performed physical modeling of the transient response with multiple (up to 1000 times) field excitations and signal accumulation in order to check whether additional magnetization arises during soundings, and found out that the average accumulated emf agrees with a single sampling within the uncertainty.

The reported pattern of the field radial component and the possibility of its duplication when using two horizontal loops with opposite moments as the current source (Epov et al., 2003b) prompted us to investigate the TEM response with the configuration shown in Fig. 4. It consists of four vertical receiver loops with $r_0 = r_k$ positioned in a circle at a distance r_k from z. The transmitter loops are spaced at $l = 2r_k = 46$ mm along z.

Figure 5, *a* shows the behavior of emf at different inner radii. Inner radius changes greater than $0.125h$ (h is wall thickness in mm) can be detected if the available processing algorithms can resolve a signal of 1 μV against the noise. Therefore, it is possible to detect 1 mm thinning of an 8 mm thick wall within a depth interval at least 100 mm.

The effect of magnetic permeability on emf is such that at late times a μ decrease is equivalent to h decrease and μ increase can be interpreted as h increase.

Note that at different μ, the TEM curves have a characteristic time t^* where emf does not change (Fig. 5, *b*): emf is inversely proportional to μ at $t < t^*$ and directly proportional to it at $t > t^*$. The time t^* depends on the thickness h. It is 10 ms for the thickest wall ($h = 8$ mm) and 1 ms at $h = 2$ mm. Therefore, the time t^* in the TEM curves can indicate changes in metal magnetic permeability and its value depends on the wall thickness.

At late times, emf is more sensitive to wall thinning than to magnetic permeability, and hence, for example, the μ change from 60 to 120 causes an h error no greater than 0.5 mm; the error can reach 25% at $h = 8$ mm.

In the real TEM curves, emf changes up to 30% in different string segments, which has been attributed to magnetic permeability changes. Forward numerical solutions show that

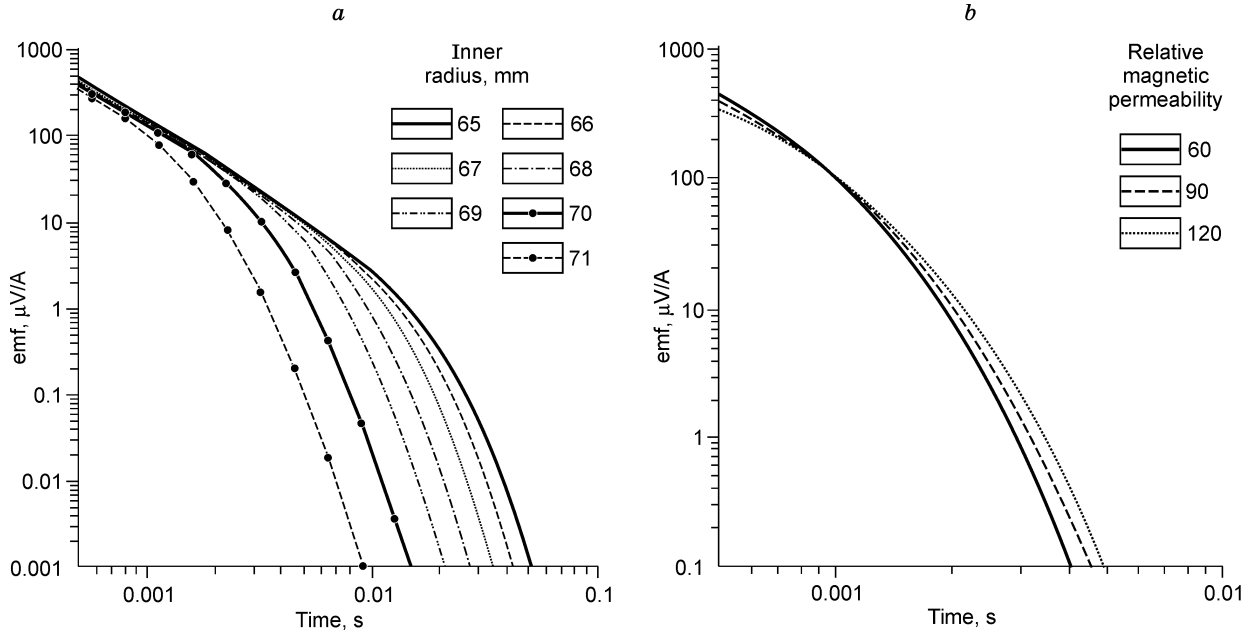

Fig. 5. TEM response of vertical loops to changes in cylinder inner radius (*a*) and in cylinder magnetic permeability (*b*).

magnetic permeability of strings can likewise change no more than 30%. Then, h error caused by μ changes will be less than 1 mm.

The TEM response in the configuration with vertical receiver loops is more sensitive to inner radius changes than in the case of horizontal loops. The response of emf to μ — t^* changes in a radial loop configuration is shifted to later times which makes it possible to estimate the string inner radius at early times. This complex behavior of emf at different parameters of the conducting ferromagnetic string obviously calls for including the forward modeling blocks into field data processing.

Field excitation by a complex source signal

We investigated the TEM response to a source signal of a complex shape in order to reduce the effect of magnetic permeability on the recorded signal and to separate in time the effects of radius and magnetic permeability changes.

It is known that the response to excitation by a signal of the duration Δt is $f^p(t) = f^s(t) - f^s(t + \Delta t)$, where $f^s(t)$ is the step field. The response to excitation by a complex signal consisting of two rectangular pulses — a positive one of the duration Δt_1 and a negative one of the duration Δt_2 that immediately follows the positive pulse — is given by

$$f^p(t) = -f^s(t) + 2f^s(t + \Delta t_1) - f^s(t + \Delta t_1 + \Delta t_2).$$

We modeled the transient responses to complex signals with their negative components from 25 to 150 ms at magnetic permeabilities from $60\mu_0$ to $120\mu_0$.

Comparison of responses to signals with different durations of the negative component shows that the effect of magnetic permeability can be reduced no more than 30% at $t < 50$ μs. This is essential for flaw detection in casing strings as it reduces the effect of variable magnetic permeability in metals.

At greater durations of the positive signal component, from 3.75 to 15 ms in our case, the response amplitude increases by a factor of 1.5 to 2. In practice the choice of signal duration depends on technical requirements (e.g., duration of a measurement cycle or logging time, etc.).

The emf behavior and its response to wall thickness changes are almost the same for the step and complex signals (see Fig. 6).

According to the μ-dependent distribution of current density in string walls, induction current concentrates ever more near the inner wall and diffuses over the wall thickness at ever later times as magnetic permeability increases. Therefore, the area of the greatest h sensitivity at great μ corresponds to much weaker responses.

As in the case of the TEM response to step excitation, the responses to the complex signal at greater μ and h are the same.

Thus, the complication of the source signal shape does not reduce much the effect of magnetic permeability on the recorded field.

Responses of a harmonic field to changes in string parameters

Thus, we found out that the times between 10^{-5} and 0.1 s are the best for emf measurements. Yet, the corresponding

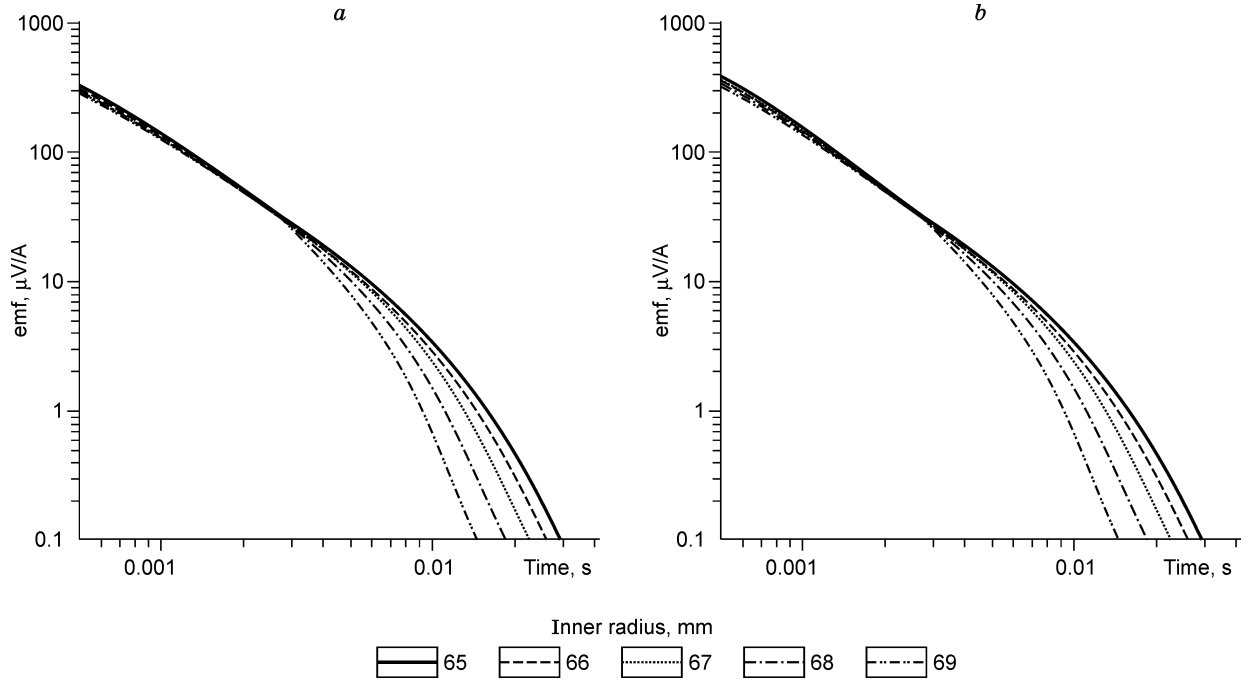

Fig. 6. TEM response to excitation by complexly-shaped (*a*) and step (*b*) signals. Relative magnetic permeability μ = 90.

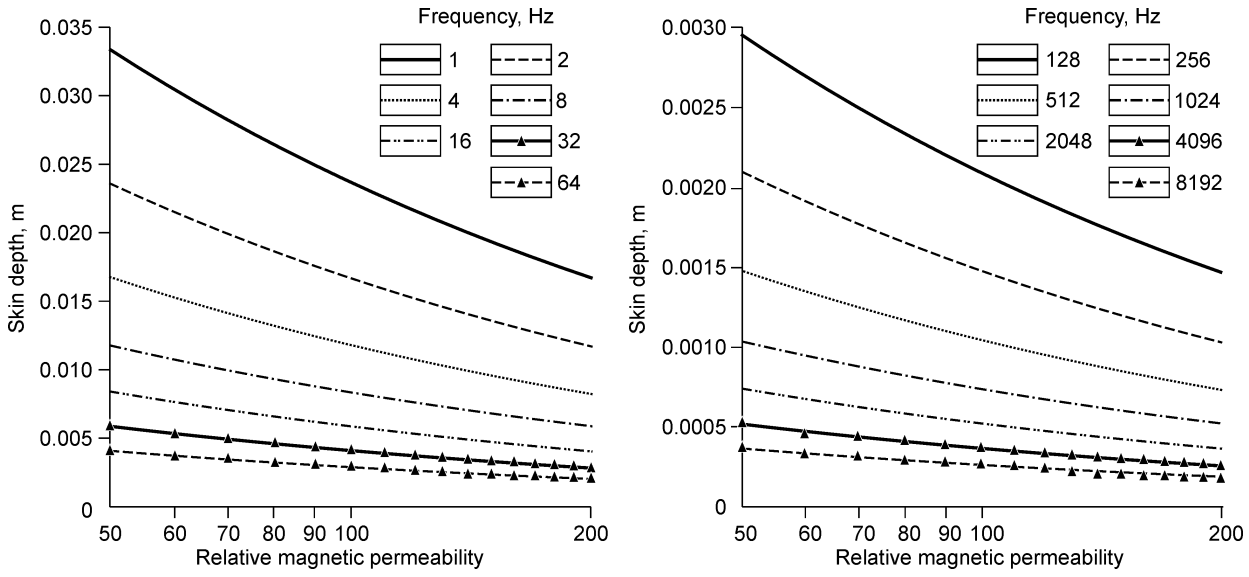

Fig. 7. Skin depth as a function of relative magnetic permeability.

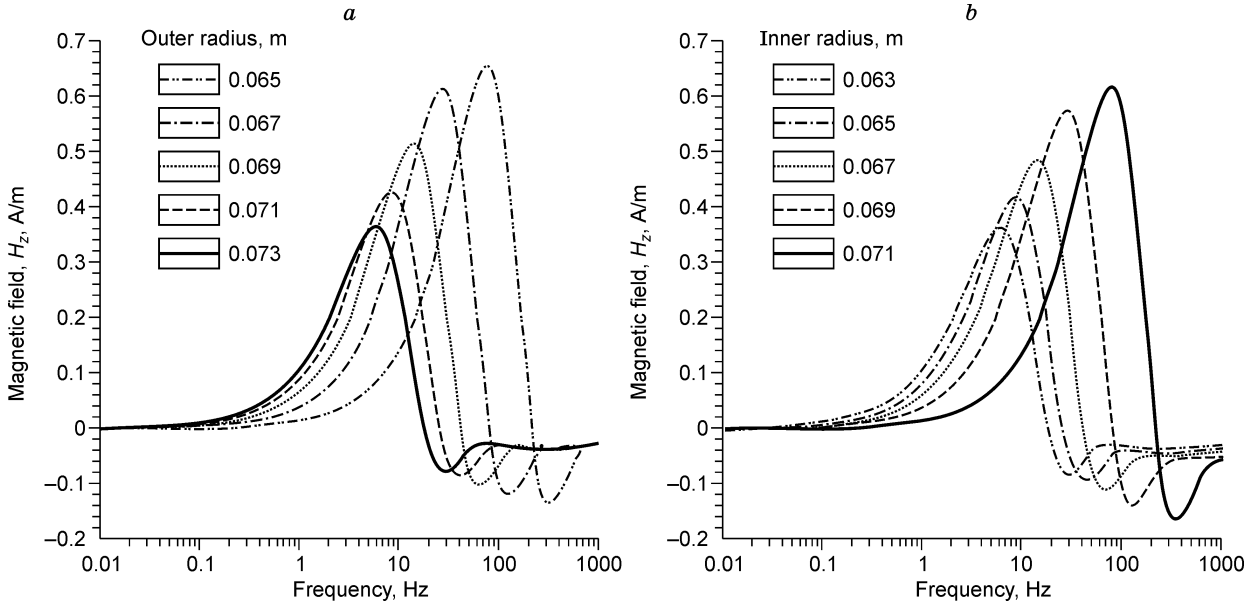

Fig. 8. Response of harmonic field to changes in wall thickness. *a* — changing outer radius (r_1 = 0.063 m); *b*— changing inner radius (r_2 = 0.073 m).

frequency band, from 0.1 to 100 kHz, is noisy. The available noise reduction techniques imply filtering at early and late times, filtering of technological and pulse noise, etc. It appears, however, easier to provide noise immunity using monochromatic source signals and narrow-band filters in receivers.

The required band is controlled by the rate of current penetration through the string wall. Figure 7 shows the skin depth at a resistivity of $2.2 \cdot 10^{-7}$ Ohm·m and magnetic permeabilities from 50 to $200\mu_0$. The depth of 0.01 m, corresponding to the wall thickness in many strings (Epov et al., 2003a), commands a band of 1 to 1000 Hz (Fig. 7). The plots in Fig. 8 show the response of the harmonic field to changes in the thickness *h* at different inner and outer string radii, at a separation of 0.3 m. The field peaks to 0.4–0.7 A/m at 1–100 Hz where it depends uniquely on *h* (Fig. 8). Within the same band, the field is highly sensitive to changes in the string magnetic permeability (Fig. 9). The μ resolution is high in the vicinity of the most probable values $\mu \sim 100\mu_0$.

Note that the field is inversely proportional to μ, though the frequencies from 1 to 100 Hz are very low in geophysical applications. In the case of common rocks with resistivities above a few Ohm·m and magnetic permeabilities about μ_0, magnetic field within this band obeys the laws of the small parameter domain $p = \omega\mu r/\rho$. The *p* expansion of emf (Kaufman, 1965) at p = 0.01–0.08 shows that the harmonic field along the well axis is proportional to μ. At the magnetic permeability of the metal magnetic cylinder $\mu \approx 100\mu_0$ and the

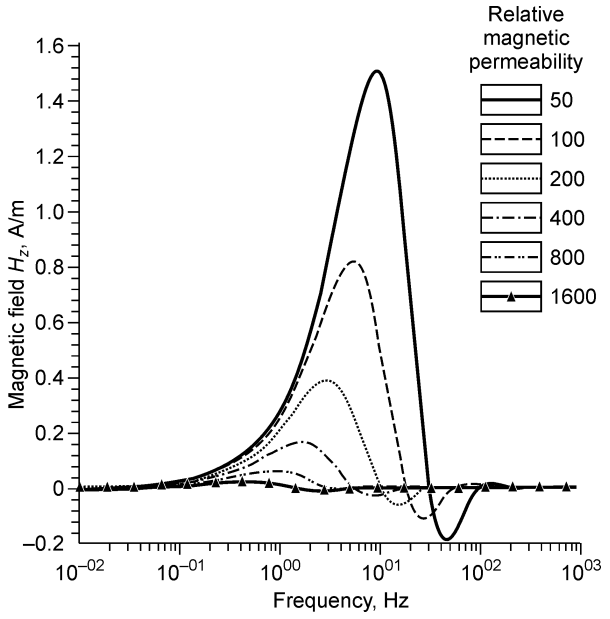

Fig. 9. Response of harmonic field to changes in magnetic permeability.

resistivity $\rho \approx 10^{-7}$ Ohm·m, $p \approx 100\omega$, i.e., $p \approx 0.01$ is provided at ω about 10^{-4} Hz.

Therefore, the 1–100 Hz band corresponds to large p and the times below 0.001 s in the transient mode where the field is inversely proportional to μ.

The magnetic field at 1 Hz responds weakly to 8% μ changes near the average $105\mu_0$ typical of real string samples (Figs. 8 and 9). The wall thickness h and the magnetic field H are approximately related as $d\ln h \cong d\ln H$.

Thus, the use of monochromatic source signals can provide a higher sensitivity of the recorded emf to changes in string geometry and allows reducing the impact from μ. However, the practical use of low frequencies is difficult because the induced emf is very low to be measured.

Responses of stationary magnetic field to changes in string parameters

Stationary magnetic field is induced by direct current in the transmitter loop. Unlike the transient field, it depends rather on the magnetic properties and structure of the medium than on its conductance.

Therefore we investigate the responses of the stationary magnetic field to changes in string radius and magnetic permeability, which is useful in the case of dc excitation in the TEM method or in autonomous instruments for excitation and recording of magnetic field components.

In the numerical modeling we used the equations for the stationary magnetic field components from (Epov et al., 2002). Figure 10 shows the behavior of the H_z component and its sensitivity to the inner string radius at changing h and an invariable outer radius of 0.073 m. Relative error is shown for the greatest wall thickness (r_1 = 0.065 and r_2 = 0.071 m). At a distance from the source of 0.1–0.2 along z, the H_z component is 70 to 150 A/m. The increment of the magnetic field per h = 0.001 m is about 2 A/m, at a downhole instrument error of 0.02 A/m (Igolkina et al., 1999). Therefore, the inner radius can be estimated to a good accuracy, neglecting the noise and assuming invariable magnetic properties of the string.

In some magnetometers the stationary magnetic field from an air source is cancelled by an additional permanent magnet. The behavior of H_z at different magnetic permeabilities in this case is shown in Fig. 11. The μ resolution of the field is sufficient for estimating the magnetic permeability, but at a separation of 0.1 to 0.3 m the field responds to changes in both magnetic permeability and wall thickness.

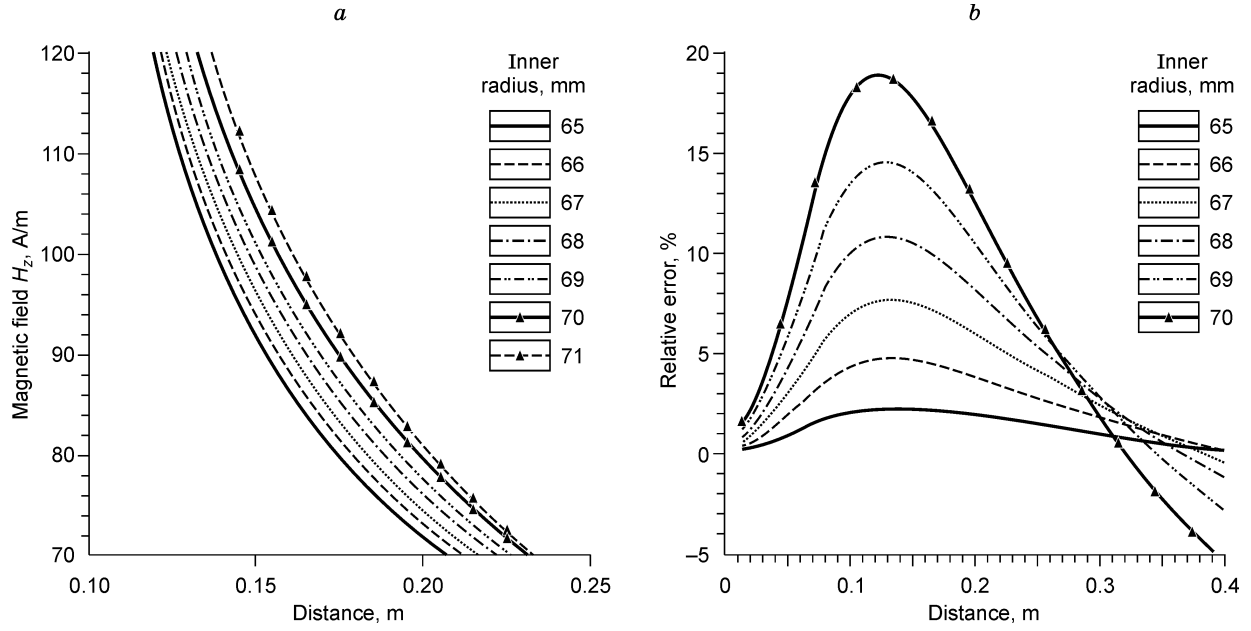

Fig. 10. Stationary magnetic field inside cylinder. *a* — behavior of H_z component at different inner radii r_1; *b* — sensitivity of H_z component to changes in inner radius r_1.

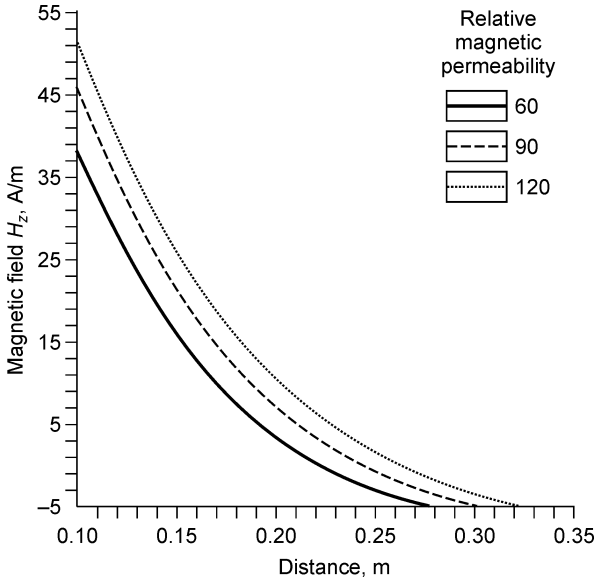

Fig. 11. Behavior of H_z-component of stationary magnetic field at different relative magnetic permeabilities (μ).

The obtained responses of the TEM and stationary magnetic fields to changes in the string geometry and electromagnetic parameters were used (i) for designing a flaw detector and technical improvements and (ii) as a background for interpretation of field data.

The inversion algorithms for the TEM responses and their tests in log data interpretation are given in (Epov et al., 2003a).

Conclusions

When recording the $\partial B_z/\partial t$ component, the wall thickness h estimated at some point z coinciding with the loop center can be attributed to any point within the interval $z \pm 1.5z_0$.

A configuration with radial receivers is highly sensitive to changes in the string inner radius. The TEM responses in this configuration bear pronounced signature of changes in string wall thickness or magnetic permeability.

The harmonic field is especially highly sensitive to the geometry of ferromagnetic conducting metal strings within the 1–100 Hz band.

References

Epov, M.I., Morozova, G.M., Antonov, E.Yu., 2002. Electromagnetic flaw detection of casing strings in petroleum wells (Fundamentals of theory and methods) [in Russian]. Geo, Izd. SO RAN, Novosibirsk.

Epov, M.I., Morozova, G.M., Antonov, E.Yu., Kuzin, I.G., 2003a. A method of non-destructive monitoring of casing strings in petroleum wells by electromagnetic soundings. Fizikotekhnicheskiye Problemy Razrabotki Poleznykh Iskopaemykh 3, 13–23.

Epov, M.I., Morozova, G.M., Mogilatov, V.S., Antonov, E.Yu., 2003b. The TEM field of a current loop centered on the axis of a conducting cylindrical layered magnet, Geologiya i Geofizika (Russian Geology and Geophysics), 44 (10), 1070–1079 (1035–1044).

Igolkina, G.V., Astrakhantsev, Yu.G., Glukhikh, I.I., Litvinov, E.P., 1999. Prospects for induction logging for studies of sedimentary sections and the Paleozoic basement of West Siberia, from deep drilling results, in: Epov, M.I. (Ed.), Electrical and electromagnetic studies in petroleum wells [in Russian]. UIGGM, Novosibirsk, 291–298.

Kaufman, A.A., 1965. Theory of induction logging [in Russian]. Nauka, Novosibirsk.

Martynov, A.S., Polygalov, V.F., Epov, M.I., Morozova, G.M., Mogilatov, V.S., 1999. Creating an electromagnetic scanner of casing strings: Technical aspects, in: Epov, M.I. (Ed.), Electrical and electromagnetic studies in petroleum wells [in Russian]. UIGGM, Novosibirsk, 91–102.

Morozova, G.M., Polygalov, V.F., Epov, M.I., Mogilatov, V.S., 2000. Transient electromagnetic field of a current loop centered on the axis of a hollow magnetic cylinder (problem solution and applications), Geologiya i Geofizika (Russian Geology and Geophysics), 41 (11), 1492–1500 (1435–1444).

Vonsovsky, S.V., Shur, Ya.S., 1948. Ferromagnetism [in Russian]. Gostekhteorizdat, Moscow-Leningrad.